Contribution from the Laboratoire de Spectrochimie des Elément de Transition, Equipe de Recherche Associée au CNRS, No. 672, Université de Paris-Sud, 91405 Orsay, France, and the Laboratoire de Chimie de Coordination du CNRS, Associé à l'Université Paul Sabatier, 31400 Toulouse, France

Crystal Structures, Magnetic Anisotropy Properties, and Orbital Interactions in *catena*-(μ-Nitrito)-bis(ethylenediamine)nickel(II) Perchlorate and Triiodide

ANNE MEYER,[1a] ALAIN GLEIZES,[1b] JEAN-JACQUES GIRERD,[1a] MICHEL VERDAGUER,[1a] and OLIVIER KAHN*[1a]

Received January 6, 1981

The crystal structures of the two title compounds $(Ni(en)_2NO_2)ClO_4$ and $(Ni(en)_2NO_2)I_3$ were solved at room temperature. The former crystallizes in the orthorhombic system, space group *Pnma*. Its lattice constants are $a = 15.223$ (4) Å, $b = 10.300$ (3) Å, and $c = 8.295$ (2) Å with $Z = 4$. Least-squares refinement of the structure has led to an R factor of 0.028. The latter crystallizes in the orthorhombic system, space group *Pmma*, the lattice constants being $a = 17.845$ (3) Å, $b = 5.232$ (1) Å, and $c = 8.237$ (1) Å with $Z = 2$. Least-squares refinement has led to $R = 0.047$. Both structures consist of infinite chains $(Ni(en)_2NO_2)$ with Ni(II) ions aligned along the b axis and bridged by NO_2 groups in an asymmetric manner, separated by ClO_4^- or I_3^- counteranions. The shortest intrachain Ni–Ni distance is 5.150 Å in the perchlorate and 5.232 Å in the triiodide. Both structures are strongly disordered. The temperature dependences of the three principal susceptibilities of $(Ni(en)_2NO_2)ClO_4$ were measured in the 3.8–300 K temperature range. They exhibit a maximum around 62 K characteristic of a strong intrachain antiferromagnetic coupling. In the 50–300 K temperature range, the weak observed magnetic anisotropy is attributed to the anisotropy of the crystal **g** tensor. Below 50 K, the magnetic anisotropy remains nearly axial but becomes much more important owing to the local anisotropy (ZFS) around each Ni(II) ion. The exchange parameter of the isotropic Heisenberg Hamiltonian $-J\sum_{i=1}^{N}\hat{S}_i\cdot\hat{S}_{i+1}$ $(N \rightarrow \infty)$ was found equal to -33.0 cm^{-1}, and the D axial parameter of the ZFS term $D\sum_{i=1}^{N}S_{iz}^2$ was estimated as 0.6 cm^{-1}. For $(Ni(en)_2NO_2)I_3$, the magnetic study was limited to the measurement of the average susceptibility. J was then found equal to -31.9 cm^{-1}. The strong antiferromagnetic coupling observed in both compounds was interpreted from the Kahn–Girerd–Charlot orbital model valid for chains of paramagnetic ions without first-order orbital momentum. The interaction of the z^2-type magnetic orbitals along the chain leads to a molecular orbital band, the width of which is related to the magnitude of the antiferromagnetic coupling. The top of the band corresponds to a MO strongly antibonding with regard to the metal d orbitals whereas the bottom of the band corresponds to an essentially nonbonding interaction of the d_{z^2} metal orbitals.

Introduction

For about half a decade, a large part of the activity of our laboratory[1a] has been devoted to the study of the interaction between paramagnetic metal ions in coupled systems, including linear chains. One of the themes we developed more specifically in this frame is the achievement of strong interaction between metal ions relatively far away from each other through extended bridging ligands.[2,3] In this respect, spectacular results can be obtained with Cu(II) polymetallic complexes,[2,4] which generally are not transposable to the other metal ions. However, our attention was drawn by the compounds $(Ni(en)_2NO_2)X$ with en = ethylenediamine and $X = ClO_4$ or BF_4. Two papers had already been devoted to the determination of the crystal structures.[5,6] Both pointed out that the compounds were formed out of $(Ni(en)_2NO_2)$ chains separated by X^- counteranions, the Ni(II) ions being bridged along the chain by NO_2 groups. However the latter paper[6] modified the conclusions of the former[5] for the coordination of the NO_2^- bridges. Whereas the spectroscopic properties (infrared, UV, and visible) of these compounds and of related complexes were extensively investigated,[7–9] the already performed magnetic measurements[5,7,8] were carried out on powder samples and limited to the temperature range 80–300 K. Nevertheless, they suggested that the nearest-neighbor Ni(II) ions along the chain were strongly coupled in an antiferromagnetic manner, in spite of the large Ni–Ni separation. This is why we decided to reinvestigate this problem. Although the latter crystal structure determination[6] seemed to us correct in its broad outlines, we preferred to refine this structure up to a very good agreement factor in order to eliminate any doubt as to the coordination of the NO_2^- bridges. Then, the temperature dependences of the three principal magnetic susceptibilities were measured down to 3.8 K for both the perchlorate and the tetrafluoroborate compounds. These measurements allowed an accurate determination of the magnitude of the intrachain exchange. They also led to the sign and an estimation of the magnitude of the local anisotropy around each metal ion. The last but not the least step of this work consisted of the study of the orbital mechanism of the intrachain interaction.

During this work, we also prepared several other $(Ni(en)_2NO_2)X$ compounds with the same chain structure. For $X = ClO_4$, BF_4, or PF_6, the compounds are isomorphous. It is no longer true for $X = I_3$. Then, we included in this paper the crystal structure and the powder magnetic properties of $(Ni(en)_2NO_2)I_3$.

Experimental Section

Syntheses. $(Ni(en)_2NO_2)ClO_4$ was prepared by mixing stoichiometric amounts of $Ni(en)_2(H_2O)_2(ClO_4)_2$ obtained according to ref 10 and sodium nitrite in aqueous solutions. Well-shaped red single crystals suitable for both X-ray and magnetic anisotropy studies were obtained by slow evaporation. The crystals were washed with methanol and dried under vacuum.

$(Ni(en)_2NO_2)X$ with $X = BF_4$ or PF_6 were prepared by mixing stoichiometric amounts of $Ni(en)_2(NO_2)_2$ obtained according to ref 11 and $NaBF_4$ or NH_4PF_6 in aqueous solutions. Well-shaped red

(1) (a) Laboratoire de Spectrochimie des Eléments de Transition, Université de Paris-Sud. (b) Laboratoire de Chimie de Coordination, Université Paul Sabatier.
(2) C. Chauvel, J. J. Girerd, Y. Jeannin, O. Kahn, and G. Lavigne, *Inorg. Chem.*, **18**, 3015 (1979), and references therein.
(3) O. Kahn, M. Verdaguer, J. J. Girerd, J. Galy, and F. Maury, *Solid State Commun.*, **34**, 971 (1980).
(4) Y. Agnus, R. Louis, and R. Weiss, *J. Am. Chem. Soc.*, **101**, 3381 (1979).
(5) F. J. Llewellyn and J. M. Waters, *J. Chem. Soc.*, 3845 (1962).
(6) M. G. B. Drew, D. M. L. Goodgame, M. A. Hitchman, and D. Rogers, *Chem. Commun.*, 477 (1965).
(7) B. J. Hathaway and R. C. Slade, *J. Chem. Soc. A*, 952 (1967).
(8) D. M. L. Goodgame, M. A. Hitchman, and D. F. Marsham, *J. Chem. Soc. A*, 259 (1971).
(9) J. R. Ferrado and L. Fabbrizzi, *Inorg. Chim. Acta*, **26**, L15 (1978).
(10) M. E. Farago, J. M. James, and V. C. G. Trew, *J. Chem. Soc. A*, 820 (1967).

0020-1669/82/1321-1729$01.25/0

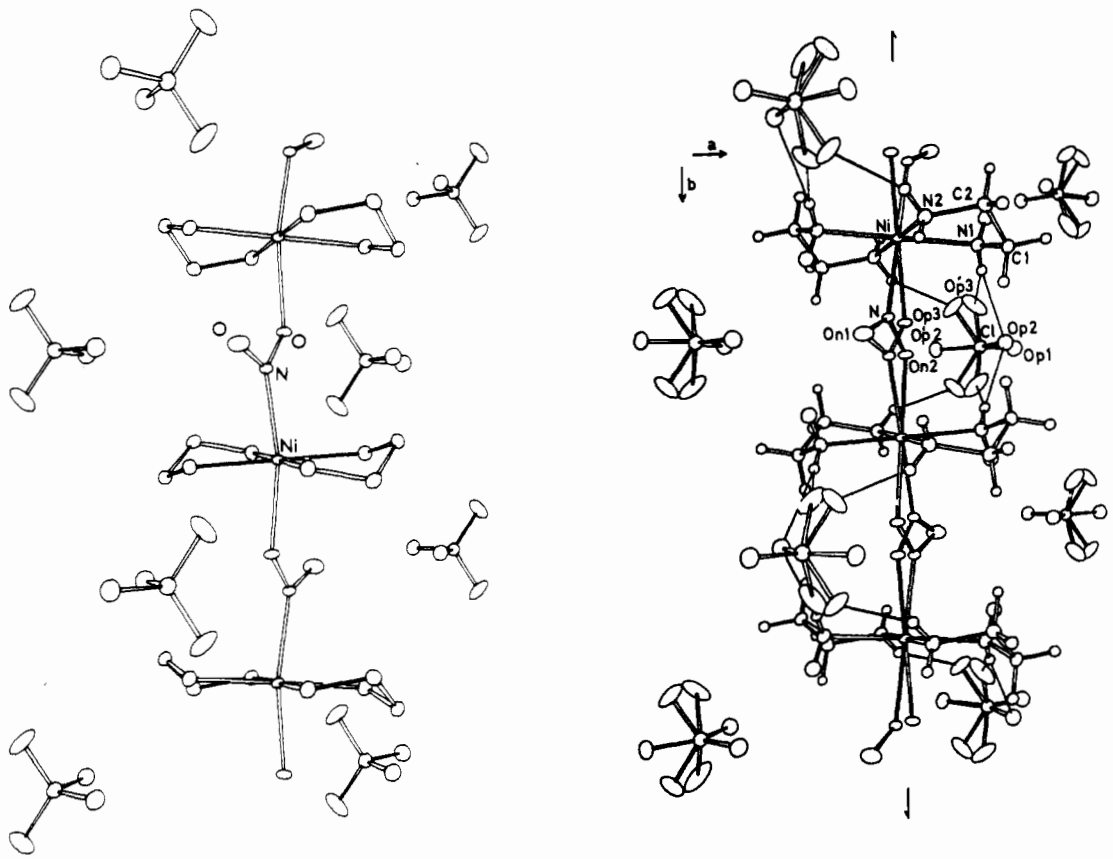

Figure 1. (Right) View of the structure of $(Ni(en)_2NO_2)ClO_4$ with 10% probability thermal ellipsoids. The two possible chain orientations are drawn, one being darkened for the sake of clarity. The disorder of the perchlorate anion is also represented; single lines are for H bonds. (Left) View of the structure without the disorder.

single crystals were obtained by slow evaporation. They were washed with methanol and dried under vacuum.

$(Ni(en)_2NO_2)I_3$ was prepared according to the reaction[12] $Ni(en)_2(NO_2)_2 + KI + I_2 \rightarrow (Ni(en)_2NO_2)I_3 + KNO_2$ with a large excess of NO_2^- and Ni^{2+} ions to avoid the formation of $Ni(en)_2(I_3)_2$ and $Ni(en)_3I(I_3)$ during the crystallization. The ion $Ni(en)_3^{2+}$ can be formed from $Ni(en)_2^{2+}$ due to the equilibrium $3Ni(en)_2^{2+} \rightleftarrows 2Ni(en)_3^{2+} + Ni^{2+}$. We operated as follows: 2.5×10^{-3} mol of $Ni(en)_2H(NO_2)_2$, 2.5×10^{-3} mol of $NaNO_2$, and 2.5×10^{-4} mol of $NiSO_4 \cdot 7H_2O$ were dissolved in 100 mL of methanol. A 2.5×10^{-3} mol quantity of KI and 2.5×10^{-3} mol of I_2 were dissolved in 75 mL of ethanol. When the two solutions were mixed, an ochre precipitate of $(Ni(en)_2NO_2)I_3$ was deposited. This precipitate was filtered. Well-shaped very small single crystals of $(Ni(en)_2NO_2)I_3$ were obtained by slow evaporation of the filtrate.

In all the cases, the chemical analyses were carried out on all the elements but oxygen. They gave excellent agreements between calculated and found percentages.

X-ray Studies. Preliminary precession photographs showed *mmm* Laue symmetry for the three compounds $(Ni(en)_2NO_2)X$ with X = ClO_4, PF_6, or I_3; $(Ni(en)_2NO_2)PF_6$ and $(Ni(en)_2NO_2)ClO_4$ are isomorphous with nearly equal parameters (Table I), and the systematic absences are consistent with space group *Pnma* or $Pn2_1a$ as previously found by Llewellyn and Waters[5] for $(Ni(en)_2NO_2)ClO_4$ and $(Ni(en)_2NO_2)BF_4$. On the other hand, $(Ni(en)_2NO_2)I_3$ also exhibits *mmm* Laue symmetry but different cell constants (Table I). At first sight, reflections with $h + l$ odd are extinct, which would indicate a *B* face-centered lattice; however, on examination of diffractometer data, many of these reflections turned out to be weak but not absent (see below). The statistical tests showed centrosymmetric space groups.

Single crystals of the three compounds were mounted on an Enraf-Nonius CAD-4 computer-controlled four-circle diffractometer. Accurate unit-cell constants were derived from least-squares refinements of the setting angles of 25 reflections (Table I).

Table I. Crystallographic Data

	$Ni(N_2C_2H_8)_2(NO_2)(PF_6)$	$Ni(N_2C_2H_8)_2(NO_2)(ClO_4)$	$Ni(N_2C_2H_8)_2(NO_2)(I_3)$
cryst syst	orthorhombic	orthorhombic	orthorhombic
space group	*Pnma-Pn2₁a*	*Pnma-Pn2₁a*	*Pmma-Pm2a-P2₁ma*
a, Å	15.451 (2)	15.223 (4)	17.845 (3)
b, Å	10.328 (1)	10.300 (3)	5.232 (1)
c, Å	8.980 (1)	8.295 (2)	8.237 (1)
V, Å³	1433.0	1300.6	769.0
mol wt	369.88	324.36	605.63
Z	4	4	2
ρ_x, g cm^{-3}	1.71	1.66	2.62

Intensity measurements were made for $(Ni(en)_2NO_2)ClO_4$ and $(Ni(en)_2NO_2)I_3$, in the form *hkl*, with use of graphite-monochromatized Mo Kα radiation. Features of the data collections are summarized in Table II. The data were processed[13] with ignorance factors *p* of 0.04 for $(Ni(en)_2NO_2)ClO_4$ and 0.02 for $(Ni(en)_2NO_2)I_3$ in the estimation of standard deviations and were corrected for absorption (Table II).

Structure Refinements. Refinements of the two structures were performed by full-matrix least-squares techniques.[13] Throughout the refinement the function minimized was $\sum w(|F_o| - |F_c|)/\sum|F_o|$ where $|F_o|$ and $|F_c|$ are the observed and calculated structure amplitudes and the weight *w* is $4F_o^2/[\sigma(F_o^2)]^2$. The reliability coefficients are defined as $R = \sum(||F_o| - |F_c||)/\sum|F_o|$ and $R_w = (\sum w(|F_o| - |F_c|)^2/\sum wF_o^2)^{1/2}$.

(11) A. V. Babaeva and Chzhan Shou-Gan, *Russ. J. Inorg. Chem.* (*Engl. Transl.*), **5**, 1055 (1960).
(12) I. B. Baranovskii and V. I. Belova, *Russ. J. Inorg. Chem.* (*Engl. Transl.*), **10**, 162 (1965).

(13) All calculations have been performed with use of the CII-Iris-80 computer of the "Centre Interuniversitaire de Calcul de Toulouse". In addition to various local programs, modified versions of the following ones were employed: Ibers' AGNOST absorption program, which includes both the Coppens–Leiserowtz–Rabinovich logic for Gaussian integration and the Tompa analytical method; Zalkin's FORDAP Fourier summation program; Johnson's ORTEP thermal ellipsoid plotting program; Busing and Levy's ORFFE error function program; Ibers' NUCLS full-matrix least-squares program, which in its nongroup version resembles the Busing and Levy ORFLS program.

Table II. Data Collection

General Conditions
temp: 294 K
radiation: molybdenum, $\lambda(K\alpha) = 0.71069$ Å
monochromatization: oriented graphite crystal
cryst-detector dist: 207 mm
detector window: height[a] 4 mm, width[a] 4 mm

Specific Conditions for $(Ni(en)_2NO_2)ClO_4$
takeoff angle: 3.5°
scan mode: θ-2θ
max Bragg angle: 35°
scan angle: $\Delta\theta = \Delta\theta_0 + B \tan\theta$; $\Delta\theta_0$[a] = 0.90, B = 0.35
scan speed: SIGPRE[a] = 0.666, SIGMA[a] = 0.020, VPRE[a] = 20° min^{-1}, TMAX[a] = 50 s
std reflctns: 800, 002, 640, 131; checked every 3600 s
cryst morphology: monoclinic prism elongated along [010]; dimens 0.01 × 0.01 × 0.08 cm; face indices (101), ($\bar{1}0\bar{1}$), ($\bar{1}01$), ($10\bar{1}$), (010), ($0\bar{1}0$)
absorption factor: $\mu_{Mo\ K\alpha}$ = 17.27 cm^{-1}
transmission factor range: 0.753–0.885
independent reflctns collected: 2387; 1079 with $I > 3[\sigma(I)]$, 1101 with $I > 2[\sigma(I)]$

Specific Conditions for $(Ni(en)_2NO_2)I_3$
takeoff angle: 2°
scan mode: θ-θ
max Bragg angle: 26°
scan angle: $\Delta\theta = \Delta\theta_0 + B \tan\theta$; $\Delta\theta_0$[a] = 0.75, B = 0.35
scan speed: SIGPRE[a] = 0.666, SIGMA[a] = 0.018, VPRE[a] = 10° min^{-1}, TMAX[a] = 120 s
std reflctns: 200, 002, 260; checked every 3600 s
cryst morphology: hexagonal prism elongated along [010]; dimens 0.004 × 0.006 × 0.03 cm; face indices (100), ($\bar{1}00$), (101), ($\bar{1}0\bar{1}$), ($\bar{1}01$), ($10\bar{1}$), (010), ($0\bar{1}0$)
absorption factor: $\mu_{Mo\ K\alpha}$ = 72.22 cm^{-1}
transmission factor range: 0.667–0.771
independent reflctns collected: 1124; 380 with $I > 2[\sigma(I)]$, 388 with $I > 1.5[\sigma(I)]$

[a] These parameters have been defined by A. Mosset, J. J. Bonnet, and J. Galy, *Acta Crystallogr. Sect. B*, **B33**, 2633 (1977).

The atomic scattering factors for all atoms and the anomalous terms for Ni, Cl, and I atoms are from tabulations mentioned in ref 14.

$(Ni(en)_2NO_2)ClO_4$. The coordinates found by Llewellyn and Waters[5] for the nickel atom, for the carbon and nitrogen atoms of the chelating en ligands, and for the chlorine and oxygen atoms of the perchlorate anion were first refined in the space group *Pnma*, with isotropic thermal parameters. This led to R = 0.24 and R_w = 0.29. An ensuing difference Fourier map revealed the atoms of the nitrite group to be partially disordered in the same way as previously described by Drew et al.[6] for the isomorphous tetrafluoroborate derivative: the nitrogen atom N and one oxygen atom, $O_n(2)$, are "split" over two positions symmetrically related through the mirror $y = 1/4$, giving rise to two equally probable configurations for the NO_2 group, the second oxygen atom, $O_n(1)$, lying on the mirror and thus being common to both configurations (see Figure 1). One cycle of refinement including the disordered atoms of the nitrite group and isotropic thermal coefficients for all atoms yielded R = 0.13 and R_w = 0.18. These values dropped to R = 0.056 and R_w = 0.081 on introduction of anisotropic thermal parameters. Hydrogen atoms were easily located on a subsequent difference Fourier map; they were introduced in the refinement with isotropic thermal coefficients, and after one more cycle the reliability factors were R = 0.039 and R_w = 0.055. At this stage of refinement, oxygen atoms $O_p(2)$ and $O_p(3)$ of the perchlorate anion exhibited thermal coefficients B_{ii} significantly higher than those of atom $O_p(1)$. Examination of a difference Fourier map revealed as the only significant features two peaks around the perchlorate. From distance and angle calculations, these peaks could be interpreted as plausible alternative positions for atoms $O_p(2)$ and $O_p(3)$ with occupancy factors of about 20%. Further refinement, including these new extra positions for atoms $O_p(2)$ and $O_p(3)$ and their occupancy factors, led after four cycles to residuals of R = 0.028 and R_w = 0.035 for the 1101 observations with $I > 2[\sigma(I)]$ and 142 variables. In the last cycle of refinement, the highest variable-shift/esd ratio was 0.33 for nonhydrogen atoms and 0.63 for hydrogen atoms. The error in an observation of unit weight was 1.30 e. A structure factor calculation with all observed and unobserved reflections included (no refinement) gave R = 0.041. A final difference Fourier map did not show peaks higher than $1/17$th of peaks corresponding to carbon atoms in a Fourier map. Refined atomic parameters are listed in Table III. Derived root-mean-square amplitudes of vibration for the atoms are listed in Table V.

$(Ni(en)_2NO_2)I_3$. From measured intensities it appeared that only reflections $hk0$ with h odd were systematically absent, which is relevant to space groups *Pm2a*, $P2_1ma$, and *Pmma*. The use of *Pm2a* and $P2_1ma$ led to erroneous C–C and C–N bond lengths, to high correlations between parameters, and to some atoms being not stabilized. The structure was solved in space group *Pmma*.

The positions of nickel and iodine atoms were derived from a Patterson map. Consistent with the weakness of reflections with $h + l$ odd, one iodine atom and the nickel atom had to occupy special positions (2f) $1/4$, $1/2$, 0.75 and $3/4$, $1/2$, 0.25 and (2e) $1/4$, 0, 0.25 and $3/4$, 0, 0.75, respectively. The refinement of the scale factor and of the coordinates and isotropic thermal parameters of nickel and iodine atoms yielded R = 0.19 and R_w = 0.21; introducing anisotropic thermal coefficients results in R = 0.16 and R_w = 0.18.

The other nonhydrogen atoms were located on a subsequent difference Fourier map. Owing to the high symmetry, it was evident that the structure should be disordered. Indeed all the atoms of the en groups appeared in plane $y = 0$; this is not consistent with the usual nonplanar geometry of $Ni(en)_2$. On the other hand, the peaks corresponding to the nitrite group were localized in the mirrors $x = 1/4$ and $y = 1/2$ and therefore could not account for the actual geometry of NO_2. Then the problem was to determine which positions were actual atomic positions and which ones were only mean atomic positions. After several attempts, the best refinement with respect to interatomic distances, thermal motions, and R indices (R = 0.047 and R_w = 0.042) was achieved with the en group having one atom, N(2), in the mirror $y = 0$ and its three other atoms distributed over general positions around this mirror with occupancy factors equal to $1/2$; the nitrogen and one of the oxygen atoms of the nitrite group could not be distinguished from each other and were to be distributed over the same general position while the second oxygen atom could occupy two equally probable special positions in the mirror $y = 1/2$. Oxygen, nitrogen, and carbon atoms were refined isotropically.

The hydrogen atoms were given calculated positions (N–H = C–H = 0.95 Å, H–N–H = H–C–H = 109.5°) and introduced as fixed contributions with isotropic thermal parameters equal to those of atoms to which they are attached. After three cycles of refinement, the highest variable-shift/esd ratio was 0.10 and the reliability factors stabilized to R = 0.032 and R_w = 0.038 for the 388 observations with $I > 1.5[\sigma(I)]$ and 40 variables. The error in an observation of unit weight was 2.00 e. A final difference Fourier map did not show significant features. Refined atomic parameters are listed in Table IV. Derived root-mean-square amplitudes of vibrations for the iodine and nickel atoms are listed in Table V.

Magnetic Measurements. These measurements were performed in the temperature range 3.8–300 K with a Faraday-type magnetometer equipped with a He continuous-flow cryostat built by Oxford Instruments. The magnetic fields were in the range 0.5–0.6 T. Tetrakis(thiocyanato)mercury cobaltate was used as a susceptibility standard. The magnetic anisotropy measurements were made on crystals weighing about 3 mg, the crystal axes being located by a standard X-ray oscillation technique.[15] For each system, the crystals were orientated in such a way that the crystal axes were successively collinear with the rotation axis of the electromagnet, and the directions of the principal susceptibilities in the plane perpendicular to a given crystal direction were determined at room temperature by rotating the electromagnet and looking for the extremes of the susceptibilities.

(14) D. T. Cromer and J. T. Waber, "International Tables for X-ray Crystallography", Vol. IV, Kynoch Press, Birmingham, England, 1974, Table 2.2A; D. T. Cromer, *ibid.*, Table 2.3.1.

(15) M. Gerloch, I. Morgenstern-Badarau, and J. P. Audiere, *Inorg. Chem.*, **18**, 3220 (1979).
(16) C. Herring, *Magnetism*, **4** (1966), and references therein.
(17) P. W. Anderson, *Solid State Phys.*, **14**, 99 (1963), and references therein.
(18) J. Hubbard, *Proc. R. Soc. London, Ser. A*, **281**, 401 (1964), and references therein.
(19) J. J. Girerd, M. F. Charlot, and O. Kahn, *Mol. Phys.*, **33**, 1063 (1977).

Table III. Positional and Thermal Parameters for the Atoms of $Ni(N_2C_2H_8)_2(NO_2)(ClO_4)$

atom	occupancy	x	y	z	B_{11}	B_{22}	B_{33}	B_{12}	B_{13}	B_{23}
Ni		0	0	0	2.938 (15)	1.722 (12)	3.539 (18)	−0.190 (14)	0.325 (17)	−0.211 (16)
Cl		0.153 76 (6)	1/4	0.43331 (13)	4.04 (4)	4.48 (5)	4.39 (4)	0	−0.92 (4)	0
$O_p(1)$		0.224 30 (21)	1/4	0.5457 (4)	5.86 (15)	6.55 (19)	5.35 (17)	0	−2.48 (13)	0
$O_p(2)$	0.790 (11)	0.191 7 (3)	1/4	0.2710 (5)	5.74 (22)	6.3 (3)	4.02 (19)	−6.6 (3)	0.03 (15)	0
$O_p(3)$	0.790 (11)	0.105 2 (4)	0.1370 (6)	0.4452 (7)	10.4 (3)	10.0 (4)	7.56 (26)	0	−3.18 (22)	3.11 (25)
$O_p'(2)$	0.210 (11)	0.073 4 (11)	1/4	0.543 (3)	4.8 (8)	6.6 (12)	14.6 (19)	8.8 (15)	3.8 (9)	−11.3 (17)
$O_p'(3)$	0.210 (11)	0.141 4 (16)	0.1398 (23)	0.3550 (28)	14.0 (17)	13.6 (21)	11.8 (16)	0	−9.2 (13)	0
$O_n(1)$		−0.059 24 (22)	1/4	−0.1792 (4)	8.64 (20)	4.30 (15)	5.06 (15)	0	−3.15 (15)	0
$O_n(2)$		0.009 91 (21)	0.2902 (4)	0.0324 (5)	4.74 (19)	1.58 (12)	4.42 (21)	0.10 (10)	−0.67 (14)	0.06 (17)
N		−0.018 75 (26)	0.2028 (4)	−0.0579 (6)	3.39 (17)	1.80 (16)	3.39 (16)	−0.14 (11)	0.98 (14)	−0.18 (10)
N(1)		0.134 88 (17)	0.0157 (3)	0.0407 (4)	3.60 (10)	4.19 (15)	4.40 (13)	−0.38 (9)	−0.10 (8)	−0.58 (10)
N(2)		0.040 66 (18)	−0.01785 (28)	−0.2376 (3)	4.00 (11)	4.46 (14)	3.86 (11)	−0.20 (10)	0.29 (9)	−0.17 (10)
C(1)		0.177 33 (17)	0.0409 (3)	−0.1147 (4)	3.24 (11)	3.80 (11)	6.23 (18)	−0.30 (10)	0.78 (11)	0.41 (13)
C(2)		0.135 34 (19)	−0.0435 (3)	−0.2379 (4)	4.41 (13)	4.05 (12)	4.47 (15)	0.54 (11)	1.22 (11)	−0.10 (12)

atom	x	y	z	B, Å^2	atom	x	y	z	B, Å^2
H(1)N(1)	0.1442 (18)	0.073 (3)	0.106 (4)	2.3 (7)	H(1)C(1)	0.2397 (20)	0.0235 (27)	−0.109 (4)	2.5 (7)
H(2)N(1)	0.1519 (24)	−0.058 (5)	0.079 (5)	4.9 (11)	H(2)C(1)	0.1680 (17)	0.130 (3)	−0.141 (4)	2.6 (7)
H(1)N(2)	0.0094 (17)	−0.075 (4)	−0.290 (4)	2.7 (8)	H(1)C(2)	0.1576 (21)	−0.030 (3)	−0.338 (5)	3.0 (7)
H(2)N(2)	0.0300 (20)	0.038 (3)	−0.299 (4)	2.3 (8)	H(2)C(2)	0.1452 (16)	−0.133 (3)	−0.211 (4)	2.0 (6)

[a] Estimated standard deviations in the least significant figure(s) in this and subsequent tables are given in parentheses. The form of the anisotropic thermal ellipsoid is $\exp[-(^1/_4)(B_{11}h^2a^{*2} + B_{22}k^2b^{*2} + B_{33}l^2c^{*2} + 2B_{12}hka^*b^* + 2B_{13}hla^*c^* + 2B_{23}klb^*c^*)]$.

This procedure allows the obtainment of two independent determinations of each of the principal susceptibilities. In all the cases, these two determinations agreed within 2%. The average magnetic susceptibilities were obtained on powder samples of about 5 mg. The temperature was measured with a gold + 0.03% iron/chromel thermocouple calibrated at 4.2, 77.2, and 300 K. The uncertainty on the temperature is less than 0.1 K, and the uncertainty on the susceptibility is about 40×10^{-6} cm^3 mol^{-1}. All the observed susceptibilities were corrected of the diamagnetism estimated from Pascal's tables [$(Ni(en)_2NO_2)ClO_4$ -146×10^{-6} cm^3 mol^{-1}, $(Ni(en)_2NO_2)BF_4$ -153×10^{-6} cm^3 mol^{-1}, $(Ni(en)_2NO_2)I_3$ -254×10^{-6} cm^3 mol^{-1}, $(Ni(en)_2NO_2)PF_6$ -190×10^{-6} cm^3 mol^{-1}] and of the TIP estimated at 100×10^{-6} cm^3 mol^{-1} for all the complexes.

Description of the Structures

$(Ni(en)_2NO_2)ClO_4$. Main bond lengths and angles are given in Table VI. The labeling of atoms appears in Figure 1. This structural analysis shows that the crystal structure of $(Ni(en)_2NO_2)ClO_4$ is identical with that of $(Ni(en)_2NO_2)BF_4$ as previously reported by Drew et al.[6] In either compound the most interesting feature is the presence, along the twofold screw axis, of infinite chains in which nitrite groups and nickel atoms alternate following the sequence ...Ni–NO_2–Ni–NO_2.... In these chains the nitrite group is bound to a nickel atom by its nitrogen atom (Ni–N = 2.163 (4) Å) and to the next nickel atom by one of its oxygen atoms (Ni–$O_n(2)$ = 2.183 (4) Å) (Figure 1).

A disorder arises in the chains because of two possible orientations for the nitrite group. From space group considerations, this disorder may be interpreted in only one way: as the space group is either *Pnma* or $Pn2_1a$, an ordered chain must have at least a twofold axis as an element of symmetry. This means necessarily that an ordered chain does adopt either the "black" or the "white" configuration as illustrated in Figure 1 and, consequently, that the environment of a nickel atom is not centrosymmetrical; the true space group is not *Pnma* but $Pn2_1a$, as was noticed by Drew et al.[6] However, attempts to refine the structure in the space group $Pn2_1a$ failed, as much in the case of $(Ni(en)_2NO_2)BF_4$[6] as in the compound of the present study. That the structure of $(Ni(en)_2NO_2)ClO_4$ could be refined so accurately in space group *Pnma*, without anomalous trends in the thermal motion of Ni-, nitrite-, and ethylenediamine-group atoms, suggests that not only the nitrite group but also the nickel chelate $Ni(en)_2$ has two possible, equally probable orientations; however, the two resulting conformations of the nickel environment are related through a pseudo center of symmetry lying so closely to the nickel atom that (i) chemically equivalent atoms of the possibly centrosymmetrical chelate depart from each other by much less than the experimental errors on their mean positions as found in the above refinement and (ii) the impossibly centrosymmetrical nitrite ligand alone appears to be disordered. It is reasonable to think that each chain is ordered but that the orientations are randomly distributed.

The perchlorate anions are also disordered but in a way that is not related at all to the disorder of the chains. Each of them has two possible, not equally probable orientations around the bond Cl–$O_p(1)$: the one including atoms $O_p(2)$ and $O_p(3)$ is about 4 times more frequent (occupancy factor = 0.790 (11)) than the other one, which includes atoms $O_p'(2)$ and $O_p'(3)$. Although the actual space group is $Pn2_1a$, the perchlorate anion, in both its configurations, accommodates the mirror $y = {}^1/_4$ of space group *Pnma* as an intramolecular element of symmetry. This rather surprising behavior is due to the presence of hydrogen bonds between some of the perchlorate oxygen atoms and the nitrogen atoms of the ethylenediamine groups. These bonds, represented by single lines on Figure 1, attach a perchlorate anion to two ethylenediamine groups related through the pseudomirror $y = {}^1/_4$ and force it to the mirror symmetry, so the above remark about the nickel chelate

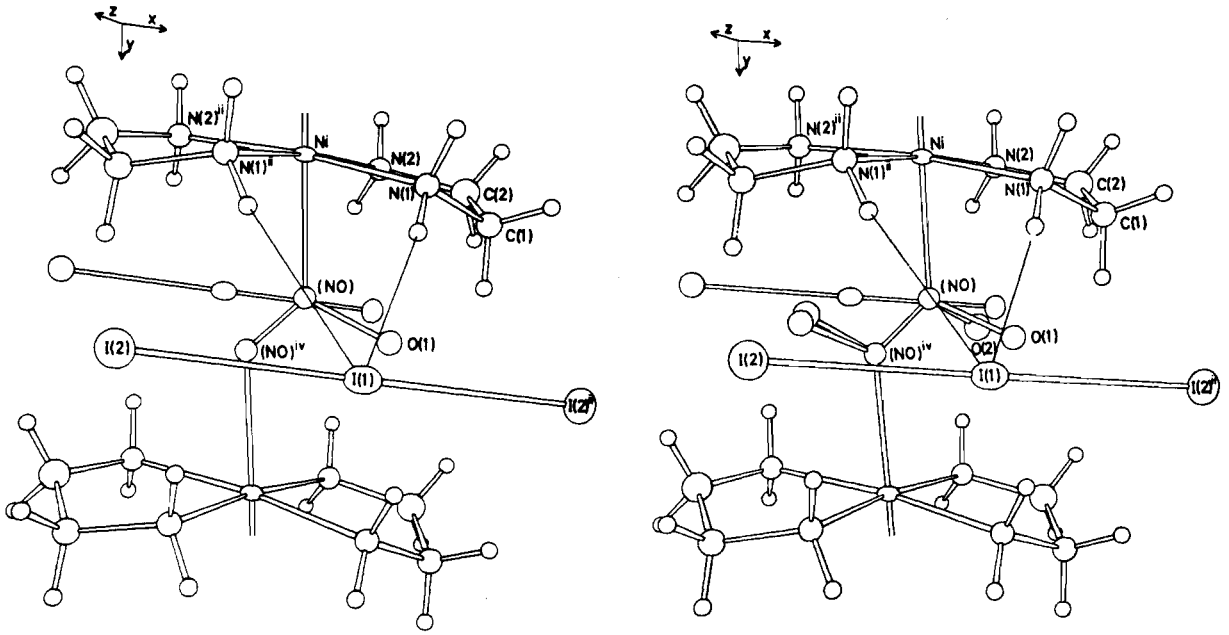

Figure 2. (Right) View of the structure of $(Ni(en)_2NO_2)I_3$ with 10% probability thermal ellipsoids. Four of the eight orientations of the nitrite group are drawn together. (NO) represents the symmetrically related positions that are occupied one by N and the other by O and vice versa. O(1) and O(2) are possible positions (not occupied at once) for the noncoordinating nitrite O atom. Hydrogen bonds are represented by simple lines. (Left) View of the structure without the disorder.

Table IV. Positional and Thermal Parameters for the Atoms of $Ni(N_2C_2H_8)_2(NO_2)(I_3)$

atom	x	y	z	B_{11}	B_{22}	B_{33}	B_{12}	B_{13}	B_{23}
Ni	1/4	0	0.2504 (6)	4.16 (9)	1.79 (6)	3.18 (8)	0	0	0
I(1)	1/4	1/2	−0.2523 (5)	7.42 (7)	3.83 (5)	3.82 (5)	0	−1.93 (10)	0
I(2)	0.08701 (6)	1/2	−0.2391 (4)	6.35 (6)	6.89 (6)	7.45 (8)	0	0	0

atom	occupancy	x	y	z	B, Å^2	atom	x	y	z	B, Å^2
N(1)	1/2	0.3315 (13)	0.035 (5)	0.0856 (13)	4.0 (4)	H(1)N(1)	0.317	0.162	0.008	4.0
N(2)	1	0.3423 (14)	0	0.4188 (13)	4.5 (4)	H(2)N(1)	0.338	−0.123	0.033	4.0
C(1)	1/2	0.4045 (12)	0.115 (5)	0.1918 (29)	4.7 (6)	H(1)N(2)	0.336	0.133	0.496	4.5
C(2)	1/2	0.4118 (13)	0.032 (13)	0.333 (3)	6.9 (8)	H(2)N(2)	0.345	−0.16	0.473	4.5
(NO)[a]	1	0.2718 (5)	0.4128 (17)	0.2718 (5)	3.77 (27)	H(1)C(1)	0.408	0.296	0.153	4.7
O(1)	1/2	0.3441 (23)	1/2	0.214 (4)	4.6 (9)	H(2)C(1)	0.443	0.038	0.100	4.7
O(2)	1/2	0.329 (3)	1/2	0.339 (6)	6.2 (10)	H(1)C(2)	0.438	0.173	0.385	6.9
						H(2)C(2)	0.440	−0.112	0.335	6.9

[a] This atom was given scattering factors intermediate between those of nitrogen and those of oxygen: $f(NO) = 1/2[f(N) + f(O)]$.

Table V. Root-Mean-Square Amplitudes of Vibration (Å)

atom	min	intermed	max
	$(Ni(en)_2NO_2)ClO_4$		
Ni	0.1458 (5)	0.1884 (6)	0.2170 (6)
Cl	0.2039 (15)	0.2383 (14)	0.2555 (2)
$O_p(1)$	0.198 (4)	0.288 (4)	0.320 (4)
$O_p(2)$	0.226 (5)	0.270 (5)	0.280 (6)
$O_p(3)$	0.211 (4)	0.270 (5)	0.486 (8)
$O_p'(2)$	0.213 (2)	0.289 (3)	0.448 (3)
$O_p'(3)$	0.123 (2)	0.264 (2)	0.644 (4)
$O_n(1)$	0.202 (4)	0.233 (4)	0.364 (4)
$O_n(2)$	0.141 (5)	0.222 (5)	0.258 (4)
N	0.150 (7)	0.204 (5)	0.211 (5)
N(1)	0.204 (3)	0.225 (3)	0.249 (4)
N(2)	0.215 (3)	0.227 (4)	0.242 (4)
C(1)	0.191 (4)	0.223 (4)	0.286 (4)
C(2)	0.195 (4)	0.231 (4)	0.269 (4)
	$(Ni(en)_2NO_2)I_3$		
Ni	0.1506 (27)	0.2007 (24)	0.2294 (24)
I(1)	0.220 (7)	0.220 (8)	0.3065 (15)
I(2)	0.2490 (21)	0.2955 (15)	0.3358 (25)

symmetry stands also for the perchlorate anion. The hydrogen bonds also account for the different probabilities of the configurations of a perchlorate anion: indeed, as can be seen in Figure 1 and from hydrogen bond lengths and angles reported in Table VI, the most frequent configuration of a perchlorate anion corresponds to the creation of four hydrogen bonds while the least frequent one corresponds to only two such bonds.

$(Ni(en)_2NO_2)I_3$. Main bond lengths and angles are listed in Table VII. The labeling of atoms appears in Figure 2. The determination of the crystal structure of $(Ni(en)_2NO_2)I_3$ shows that the linearly chained cationic framework remains unchanged on replacing the spherical anions ClO_4^- or BF_4^- by the cylindrical one I_3^- (Figure 2). It is clear that once again the overall high symmetry observed is a consequence of a disorder. But this time, the disorder is of a higher degree than in the previous compound. The nitrite group has eight possible, equally probable orientations, which correspond to four possible positions for each atom (Figure 3). The bridging oxygen and nitrogen atoms appear distributed over the same four equivalent positions, forming a rectangle whose opposite corners are 1.198 (17) Å apart. That this value departs by about 0.05 Å from the usual nitrite N–O bond lengths probably means that one observes mean positions. Therefore the Ni–O and Ni–N bond lengths that look equal, Ni–(NO) = 2.200 (9) Å, are actually not and cannot be specified. In the same way, the nitrite interatomic distances cannot be considered as the real ones.

Table VI. Bond Lengths (Å) and Angles (Deg) in $Ni(N_2C_2H_8)_2(NO_2)(ClO_4)$[a]

Area around Nickel			
Ni-N(1)	2.087 (2)	Ni-N	2.163 (4)
Ni-N(2)	2.074 (3)	Ni-$O_n(2)^{ii}$	2.183 (4)
N(1)-Ni-N(2)	82.35 (11)	N(1)-Ni-$O_n(2)^{ii}$	80.54 (13)
N(1)-Ni-N	95.23 (14)	N(1)-Ni-$O_n(2)^{iii}$	99.46 (13)
N(1)-Ni-N^i	84.77 (14)	N(2)-Ni-$O_n(2)^{ii}$	100.61 (13)
N(2)-Ni-N	85.05 (16)	N(2)-Ni-$O_n(2)^{iii}$	79.39 (13)
N(2)-Ni-N^i	95.95 (16)	N-Ni-$O_n(2)^{iii}$	156.91 (14)
Ethylenediamine Ligand			
N(1)-C(1)	1.465 (4)	N(2)-H(2)N(2)	0.78 (4)
N(2)-C(2)	1.465 (4)	C(1)-H(1)C(1)	0.97 (3)
C(1)-C(2)	1.486 (5)	C(1)-H(2)C(1)	0.95 (3)
N(1)-H(1)N(1)	0.82 (3)	C(2)-H(1)C(2)	0.91 (4)
N(1)-H(2)N(1)	0.87 (5)	C(2)-H(2)C(2)	0.96 (3)
N(2)-H(1)N(2)	0.87 (4)		
Ni-N(1)-C(1)	107.8 (2)		
Ni-N(1)-H(1)N(1)	109 (2)		
Ni-N(1)-H(2)N(1)	107 (2)		
H(1)N(1)-N(1)-H(2)N(1)	110 (4)		
H(1)N(1)-N(1)-C(1)	112 (2)		
H(2)N(1)-N(1)-C(1)	110 (3)		
Ni-N(2)-C(2)	108.1 (2)		
Ni-N(2)-H(1)N(2)	112 (2)		
Ni-N(2)-H(2)N(2)	119 (3)		
H(1)N(2)-N(2)-H(2)N(2)	93 (4)		
H(1)N(2)-N(2)-C(2)	114 (2)		
H(2)N(2)-N(2)-C(2)	109 (2)		
N(1)-C(1)-H(1)C(1)	111 (2)		
N(1)-C(1)-H(2)C(1)	108 (2)		
C(2)-C(1)-H(1)C(1)	110 (2)		
C(2)-C(1)-H(2)C(1)	110 (2)		
N(1)-C(1)-C(2)	108 (2)		
H(1)C(1)-C(1)-H(2)C(1)	110 (2)		
N(2)-C(2)-H(1)C(2)	110 (2)		
N(2)-C(2)-H(2)C(2)	109 (2)		
C(1)-C(2)-H(1)C(2)	112 (2)		
C(1)-C(2)-H(2)C(2)	109 (2)		
N(2)-C(2)-C(1)	108 (3)		
H(1)C(2)-C(2)-H(2)C(2)	107 (3)		
Nitrite Ligand			
N-$O_n(1)$	1.276 (5)	$O_n(1)$-$O_n(2)$	2.088 (4)
N-$O_n(2)$	1.249 (5)		
$O_n(1)$-N-$O_n(2)$	111.5 (3)	Ni-N-$O_n(1)$	127.4 (3)
Ni-N-$O_n(2)$	121.1 (3)	Ni-$O_n(2)^{ii}$-N^{ii}	127.9 (3)
Perchlorate Anion			
Cl-$O_p(1)$	1.422 (3)		
More Frequent Configuration			
Cl-$O_p(2)$	1.465 (4)	Cl-$O_p(3)$	1.383 (4)
$O_p(1)$-Cl-$O_p(2)$	107.7 (2)	$O_p(2)$-Cl-$O_p(3)$	106.0 (3)
$O_p(1)$-Cl-$O_p(3)$	110.9 (2)	$O_p(3)$-Cl-$O_p(3)^{ii}$	114.7 (6)
Less Frequent Configuration			
Cl-$O_p'(2)$	1.53 (2)	Cl-$O_p'(3)$	1.32 (2)
$O_p(1)$-Cl-$O_p'(2)$	102.3 (10)	$O_p'(2)$-Cl-$O_p'(3)$	100.4 (13)
$O_p(1)$-Cl-$O_p'(3)$	115.4 (7)	$O_p'(3)$-Cl-$O_p'(3)^{ii}$	118 (2)
Hydrogen Bonds			
H(1)N(1)-$O_p'(3)$	2.18 (4)	H(1)N(2)-$O_p(3)^i$	2.26 (3)
H(1)N(1)-$O_p(2)$	2.39 (3)		
N(1)-H(1)N(1)-$O_p'(3)$	149 (3)	N(2)-H(1)N(2)-$O_p(3)^i$	153 (3)
N(1)-H(1)N(1)-$O_p(2)$	171 (3)		

[a] Roman numeral superscripts refer to the following equivalent positions relative to x, y, z: (i) $\bar{x}, \bar{y}, \bar{z}$; (ii) $x, {}^1/_2 - y, z$; (iii) $\bar{x}, {}^1/_2 + y - 1, \bar{z}$.

Contrary to what observed in the perchlorate and tetrafluoroborate derivatives, the ethylenediamine ligand appears to be disordered while the anion does not, at least to a significant extent. Ni(en) moieties of a chelate are related to each other through the mirror $x = {}^1/_4$. The examination of

Table VII. Bond Lengths (Å) and Angles (Deg) in $Ni(N_2C_2H_8)_2(NO_2)(I_3)$[a]

Area around Nickel			
Ni-N(1)	1.999 (19)	Ni-(NO)	2.200 (9)
Ni-N(2)	2.153 (20)		
N(1)-Ni-$N(1)^{iii}$	94.4 (10)	N(1)-Ni-$(NO)^{ii}$	95.1 (8)
N(1)-Ni-$N(1)^{ii}$	93.5 (11)	N(1)-Ni-$(NO)^{iii}$	105.7 (8)
N(1)-Ni-$N(2)^{ii}$	174.0 (9)	N(2)-Ni-(NO)	79.43 (27)
N(2)-Ni-N(1)	83.2 (4)	N(2)-Ni-$(NO)^{ii}$	94.95 (29)
N(2)-Ni-$N(2)^{ii}$	99.8 (10)	(NO)-Ni-$(NO)^i$	157.9 (5)
N(1)-Ni-(NO)	80.4 (8)	(NO)-Ni-$(NO)^{iii}$	171.4 (7)
N(1)-Ni-$(NO)^i$	90.7 (8)		
Ethylenediamine Ligand			
N(1)-C(1)	1.505 (29)	C(1)-C(2)	1.48 (3)
N(2)-C(2)	1.44 (3)		
Ni-N(1)-C(1)	111.9 (11)	N(1)-C(1)-C(2)	113.0 (25)
Ni-N(2)-C(2)	110.0 (12)	N(2)-C(2)-C(1)	115.3 (23)
Nitrite Ligand			
(NO)-$(NO)^{iv}$	1.198 (17)	$O(1)$-$(NO)^{iv}$	2.17 (4)
(NO)-O(1)	1.45 (4)	$O(2)$-$(NO)^{iv}$	1.95 (6)
(NO)-O(2)	1.26 (5)		
$(NO)^{iv}$-(NO)-O(1)	109.7 (12)	Ni-(NO)-O(1)	116.3 (8)
$(NO)^{iv}$-(NO)-O(2)	104.7 (16)	Ni-(NO)-O(2)	122.2 (10)
Ni-(NO)-$(NO)^{iv}$	129.3 (10)		
Triiodide Anion			
I(1)-I(2)	2.9105 (11)		
I(2)-I(1)-$I(2)^{ii}$	175.72 (27)		
Hydrogen Bond			
N(1)-I(1)	3.972 (21)	H(1)N(1)-I(1)	3.0
N(1)-H(1)N(1)-I(1)	170		

[a] Roman numeral superscripts refer to the following equivalent positions relative to x, y, z: (i) $x, \bar{y}, z$; (ii) ${}^1/_2 - x, y, z$; (iii) ${}^1/_2 - x, \bar{y}, z$; (iv) ${}^1/_2 - x, 1 - y, z$.

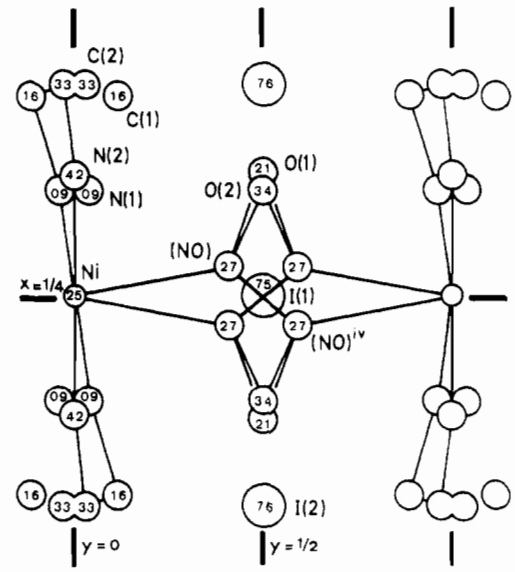

Figure 3. Partial view of the structure of $(Ni(en)_2NO_2)I_3$ projected on (001) illustrating the disorder (i) of the nitrite groups and (ii) of the $Ni(en)_2$ chelate: the boat and the chair conformations are emphasized on the left and the right sides, respectively (see text).

distances between positions that are possibly occupied by nitrogen and carbon atoms shows that in an ethylenediamine group, atoms N(1), C(1), and C(2) must be situated either all three above or all three below the mirror $x = 0$; in both cases the atom N(2) lies in the mirror. Therefore the $Ni(en)_2$ chelate may adopt two possible conformations, depending on whether ethylenediamine groups are both on the same side of the mirror (boat conformation) or one below and one above

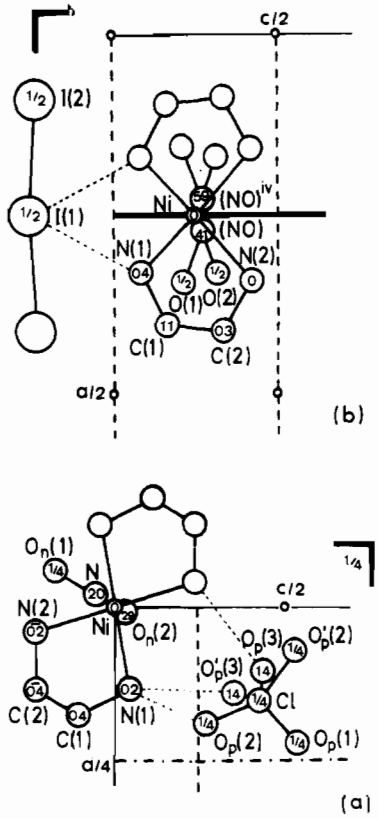

Figure 4. Partial views of the structures of $(Ni(en)_2NO_2)ClO_4$ (a) and $(Ni(en)_2NO_2)I_3$ (b) projected on (010) (see text).

the mirror (chair conformation) (Figure 3).

N–Ni–N angles corresponding to nitrogen atoms not belonging to the same ethylenediamine group are larger by about 6° on one side (N(2)–Ni–N(2) = 99.8 (10)°) than on the other side (N(1)–Ni–N(1) = 94.4 (10) or 93.5 (11)°). This distortion may be interpreted as a consequence of the hydrogen bond between atom I(1) and atom N(1), which could be responsible for the shrinkage of the angle N(1)–Ni–N(1) (Table VII, Figures 2 and 4b).

Figure 4a and b, which gives partial views of the two structures projected on (010) planes perpendicular to the chain direction, puts into evidence two major differences between $(Ni(en)_2NO_2)ClO_4$ and $(Ni(en)_2NO_2)I_3$. First, one notices that the nitrite groups are orientated in opposite ways with respect to the $Ni(en)_2$ chelates: in $(Ni(en)_2NO_2)ClO_4$ they are perpendicular to the long axis of the chelate (Figure 4a) while they are nearly parallel to that axis in $(Ni(en)_2NO_2)I_3$ (Figure 4b). Second, the nickel and the nitrite groups atoms are coplanar in the perchlorate derivative (the nickel atoms lie 0.04 Å apart from the plane of atoms $O_n(1)$, $O_n(2)$, and N); this is not the case in the triiodide derivative, as can be simply seen from Figure 4b.

Magnetic Results and Interpretation

We consider first the compound $(Ni(en)_2NO_2)ClO_4$. The thermal variations of the three principal susceptibilities χ_a, χ_b, and χ_c are represented in Figure 5. The three magnetic curves exhibit a rounded maximum around 62 K. Such a behavior is characteristic of a strong intrachain antiferromagnetic coupling. In the whole temperature range above 50 K, the magnetic anisotropy is very weak. $\chi_a - \chi_c$ varies from 50 × 10^{-6} cm^3 mol^{-1} at 300 K to 100 × 10^{-6} cm^3 mol^{-1} at 62 K. The ratio $(\chi_a - \chi_c)/\bar{\chi}$ where $\bar{\chi}$ is the average susceptibility defined as $^1/_3(\chi_a + \chi_b + \chi_c)$ is constant and equal to 1.5% between 50 and 300 K. This indicates that the susceptibility is nearly isotropic in the plane *ac* perpendicular to the axis *b* of the chain; $\chi_a - \chi_b$ varies from 250 × 10^{-6} cm^3 mol^{-1} at 300 K to

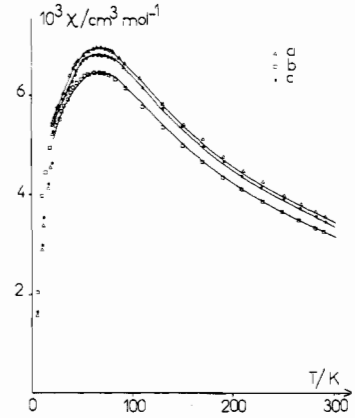

Figure 5. Experimental (□, ●, and ▲) and theoretical (—) thermal variations of the principal magnetic susceptibilities for $(Ni(en)_2NO_2)ClO_4$ (see text).

450 × 10^{-6} cm^3 mol^{-1} at 62 K. The ratio $(\chi_a - \chi_b)/\bar{\chi}$ remains around 7% between 50 and 300 K. Below 50 K, the ratios $(\chi_a - \chi_c)/\bar{\chi}$ and $(\chi_a - \chi_b)/\bar{\chi}$ are no longer constant. When the compound cools down, $\chi_a - \chi_c$ and $\chi_a - \chi_b$ diminish changing sign below 30 K. At 10 K, $\chi_a - \chi_c$ is equal to −150 × 10^{-6} cm^3 mol^{-1} and therefore remains weak. On the other hand, $\chi_a - \chi_b$ becomes equal to −1100 × 10^{-6} cm^3 mol^{-1}. In other words, the susceptibilities perpendicular to the chain axis decrease faster than the parallel susceptibility $\chi_\parallel$ when the compound cools down to very low temperatures.

In spite of the disorder of the structure, each chain is most likely ordered. But, even in case of disorder along the chain, all the bridging networks $NiNO_2Ni$ would remain strictly equivalent and the exchange parameters between nearest-neighbor ions would be equal. It turns out that the intrachain exchange may be considered as uniform. The single-ion ground term of Ni(II) in a pseudooctahedral environment is $^3A_2$ and hence has no orbital momentum at the first order. The more general spin Hamiltonian appropriate to describe the magnetic properties of Ni(II) chains is, with consideration of only the single-ion terms and the interactions between nearest-neighbor centers

$$\mathcal{H} = \sum_i (\beta \hat{S}_i \cdot g_i \cdot \vec{H} + \hat{S}_i \cdot \mathbf{D} \cdot \hat{S}_i - J\hat{S}_i \cdot \hat{S}_{i+1} + \hat{S}_i \cdot \mathbf{D}_{NiNi} \cdot \hat{S}_{i+1} + \vec{d}_{NiNi} \cdot \hat{S}_i \wedge \hat{S}_{i+1}) \quad (1)$$

where the terms represent the Zeeman perturbation, the local distortion, the isotropic exchange, the anisotropic exchange, and the antisymmetric exchange successively. S_i is the spin operator for the *i*th metal ion of the chain. Since all the metal ions are equivalent, the Zeeman perturbation may be rewritten $\hat{S} \cdot \mathbf{g} \cdot \vec{H}$ where $\hat{S}$ is now the total spin operator for the chain and $\mathbf{g}$ the crystal $\mathbf{g}$ tensor with g_u ($u = a, b, c$) principal values along the principal directions of the crystal lattice. The Hamiltonian (1) does not take into account an eventual interchain coupling that we assumed to be negligible with regard to the magnitude of the interchain coupling. This assumption may be justified by the fact that the chains are largely separated by the ClO_4^- counteranions, the nearest Ni–Ni interchain distance being 8.67 Å. It has been shown that in case of interaction between orbital singlet ions, J is by far the leading exchange term,[16-19] the components of the tensor $\mathbf{D}_{NiNi}$ and of the vector $\vec{d}_{NiNi}$ being at best of the order of a fraction of the wavenumber. Moreover, in contrast to several previously reported situations,[20-22] the exchange interaction and the local anisotropy in $(Ni(en)_2NO_2)ClO_4$ are not at all of the same

(20) T. Watanabe, *J. Phys. Soc. Jpn.*, **17**, 1856 (1962).
(21) H. T. Witteveen, W. L. C. Rutten, and J. Reedijk, *J. Inorg. Nucl. Chem.*, **37**, 913 (1975).
(22) C. Dupas and J. P. Renard, *J. Chem. Phys.*, **61**, 3871 (1974).

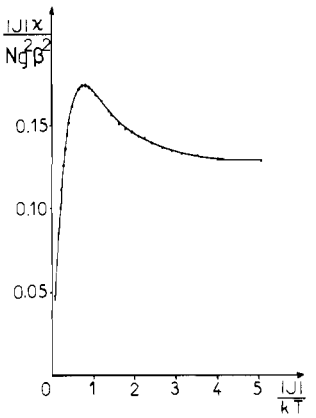

Figure 6. Comparison of Weng's values and our analytical expression for the magnetic susceptibility of infinite isotropic Heisenberg chains with $S_i = 1$.

order of magnitude, the former perturbation being much more important than the latter. Two experimental facts allow us to state this result: (i) the maximum of the susceptibilities is reached for a relatively high temperature, namely 62 K; (ii) above 50 K, the ratios $(\chi_a - \chi_b)/\bar{\chi}$ and $(\chi_a - \chi_c)/\bar{\chi}$ are nearly constant, which means that the weak magnetic anisotropy observed in this temperature range is essentially due to the anisotropy of the crystal **g** tensor. In other words, one can assert that above 50 K, the local anisotropy is largely quenched by the antiferromagnetic exchange interaction. The influence of **D**, and eventually $\mathbf{D}_{NiNi}$ and $\vec{d}_{NiNi}$, will be perceptible only at very low temperatures. It turns out that in a first step an accurate determination of J may be obtained by neglecting these contributions in (1) and by including only the magnetic data above 50 K in the fitting procedure.

There is no exact analytical expression for the temperature dependence of the susceptibility of infinite isotropic Heisenberg chains. However in the case $S_i = 1$, Weng gave results extrapolated from calculations performed on ring chains of increasing lengths.[23] To make the fitting procedure easier, we reproduced Weng's results with the analytical expression given here, which is only valid for an antiferromagnetic coupling ($J < 0$):

$$\chi_{chain} = \frac{N\beta^2g^2}{kT}\left[\frac{2 + 0.0194X + 0.777X^2}{3 + 4.346X + 3.232X^2 + 5.834X^3}\right] \quad (2)$$

with

$$X = |J|/kT$$

An expression of the same kind was proposed by Estes et al.[24] in the case $S_i = {}^1/_2$. The expression (2) is compared to Weng's results in Figure 6. The least-squares fitting of the experimental data for χ_a, χ_b, and χ_c led to

$$J = -33.0\ cm^{-1} \qquad g_a = 2.23 \qquad g_b = 2.15 \qquad g_c = 2.21$$

The agreement factor R defined by $\sum(\chi_{obsd} - \chi_{calcd})^2/\sum\chi_{obsd}^2$ is then equal to 4×10^{-4}. Experimental data and theoretical curves are compared in Figure 5. The expression (2) leads to the finite values of the susceptibility $\chi_{chain,u} \rightarrow 0.133N\beta^2g_u^2/|J|$ when $T \rightarrow 0$ whereas the experimental perpendicular susceptibilities χ_a and χ_c appear to approach zero when T approaches zero. Moreover, the magnetic anisotropy increases when the compound is cooled down to very low temperatures. If we assume that the **D** term is preponderant

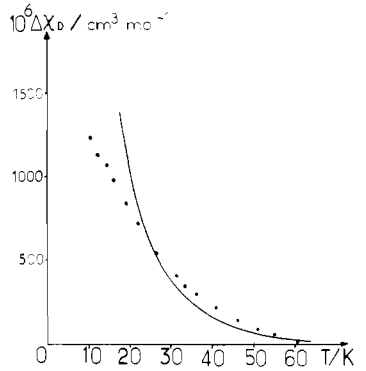

Figure 7. Experimental (●) and theoretical (—) thermal variations of the magnetic anisotropy $\Delta\chi_D$ (see text).

with regard to the $\mathbf{D}_{NiNi}$ and $\vec{d}_{NiNi}$ terms, then we can attempt to extract information on the sign and the magnitude of the local anisotropy from the low-temperature magnetic data. $\hat{S}_i\mathbf{D}\hat{S}_i$ may be reexpressed according to $D(S_{ib}^2 - {}^2/_3) + E(S_{ia}^2 - S_{ic}^2)$ where D and E are the axial (along the chain) and rhombic distortion parameters. S_{iu} ($u = a, b, c$) are the components of the spin operator along the three directions of the orthorhombic lattice. At any temperature below 50 K, $\chi_a - \chi_c$ remains weak compared to $\chi_a - \chi_b$. It turns out that the rhombic distortion is very weak with regard to the distortion along the chain, and the E parameter may be neglected. The magnetic anisotropy observed below 50 K has two origins: (i) the weak anisotropy of the crystal **g** tensor put into evidence in the range of the temperatures above 50 K; (ii) the local anisotropy essentially due to the axial distortion. Since, in this second step, we look for an estimation of this latter factor, we must correct the observed anisotropy of the crystal **g** tensor. For that, we introduced the parameter $\Delta\chi_D$:

$$\Delta\chi_D = \chi_b\frac{\bar{g}^2}{g_b^2} - \frac{1}{2}\left(\chi_a\frac{\bar{g}^2}{g_a^2} + \chi_c\frac{\bar{g}^2}{g_c^2}\right)$$

which defines the magnetic anisotropy arising from the axial local distortion. Smith and Friedberg gave an expression of $\Delta\chi_D$ for an isotropic Heisenberg chain of strongly antiferromagnetically coupled S spins. This expression, due to Griffith, must be considered at the best as a semiquantitative description of the phenomenon since it is based on the classical spin approach developed by Fisher.[26] Such an approach has a limited validity for actual $S = 1$ spins. This expression is[27]

$$\Delta\chi_D = \frac{2}{5}\frac{N\beta^2g^2}{3kT}S(S+1)\frac{DS(S+1)}{kT}F \quad (3)$$

with

$$F = \frac{(1+U)(1+V)}{(1-U)(1-V)} + \frac{2U}{1-U}$$

$$U = \coth\left[\frac{JS(S+1)}{kT}\right] - \frac{kT}{JS(S+1)}$$

$$V = 1 - \frac{3UkT}{JS(S+1)}$$

A crude agreement shown in Figure 7 is obtained for $D = 0.6\ cm^{-1}$. The sign of D means that the component $M_S = 0$ is the lowest in energy. This sign is the opposite of that obtained in Ni(II) chains made out of octahedra sharing either edges or trigonal faces.[21,28-30] To conclude this section on D,

(23) C. Y. Weng, Ph.D. Thesis, Carnegie Institute of Technology, 1968.
(24) W. E. Estes, D. P. Gavel, W. E. Hatfield, and D. J. Hodgson, *Inorg. Chem.*, **17**, 1415 (1978).
(25) T. Smith and S. A. Friedberg, *Phys. Rev.*, **176**, 660 (1968).
(26) M. E. Fisher, *Am. J. Phys.*, **32**, 343 (1964).
(27) An error appears in the expression of U given in ref 25.

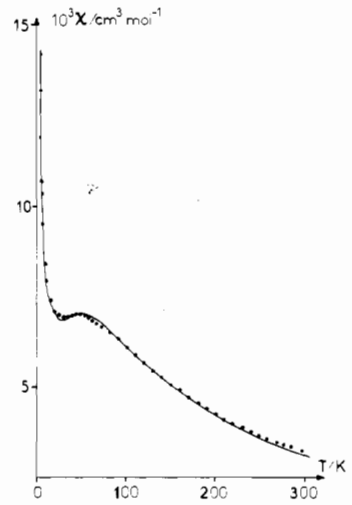

Figure 8. Experimental (●) and theoretical (—) thermal variations of the average magnetic susceptibility of $(Ni(en)_2NO_2)I_3$.

we must emphasize that if the sign of D seems to be without ambiguity, the numerical value should be regarded as tentative owing to the approximations we made and the nature of the classic spin model. Moreover, we neglected any interchain interaction. Such an interaction, even very weak, might perturb the susceptibilities observed in the liquid-helium temperature range with regard to the susceptibilities expected for perfectly isolated chains.

The same magnetic anisotropy studies were carried out with $(Ni(en)_2NO_2)BF_4$ and $(Ni(en)_2NO_2)PF_6$. In the limit of the experimental uncertainties, they gave values for J and D identical with those obtained with $(Ni(en)_2NO_2)ClO_4$.

Let us consider now $(Ni(en)_2NO_2)I_3$. All our attempts to grow single crystals suitable for magnetic anisotropy studies were unsuccessful. Therefore, we restricted ourselves to the measurement of the thermal variation of the average susceptibility. The experimental data are shown in Figure 8. When the compound cools down, the susceptibility increases up to a maximum that occurs around 48 K, decreases down to 25 K, and then increases again below 25 K. The strong antiferromagnetic coupling revealed by the maximum of the susceptibility around 48 K could be easily predicted owing to the similitude of the bridging networks of $(Ni(en)_2NO_2)I_3$ and $(Ni(en)_2NO_2)ClO_4$. The increase of the susceptibility when the compound cools down to very low temperatures is most likely due to noncoupled Ni(II) ions in the polycrystalline powder sample. The data available for $(Ni(en)_2NO_2)I_3$ do not permit an estimation of the local anisotropy parameters, more especially as the experimental points at very low temperatures essentially reflect the magnetic behavior of the noncoupled Ni(II) ions. Therefore, we interpreted the experimental data with the expression of the average susceptibility

$$\chi = \chi_{chain}(1 - \rho) + \frac{2N\beta^2g^2}{3kT}\rho \qquad (4)$$

where we take into account a proportion ρ of a monomeric impurity, of which the susceptibility is assumed to follow the Curie law $\chi_I = 2N\beta^2g^2/3kT$. χ_{chain} is the susceptibility of an infinite isotropic Heisenberg chain of $S = 1$ spins given in (2). Least-squares fitting led to the following values for the J, g, and ρ parameters:

$$J = -31.9\ cm^{-1} \qquad g = 2.12 \qquad \rho = 0.034$$

The agreement R factor is 0.9×10^{-4}. One can notice that the magnitude of the exchange interaction in $(Ni(en)_2NO_2)I_3$ is very close to what it was in $(Ni(en)_2NO_2)ClO_4$. However, the two J values have to be compared cautiously. Indeed, the one (ClO_4^-) is obtained from magnetic anisotropy measurements carried out on single crystals of very good quality; the other one is obtained from the average susceptibility measured on a polycrystalline powder containing a nonnegligible proportion of noncoupled Ni(II) ions, probably due to ends of finite chains. In this latter case, nothing allows the assertion that the expression of the susceptibility given in (4) is very good. The fact that such an expression has been extensively used up to now is in no way a definitive proof of its validity.[31] As far as the methodology of the magnetism is concerned, it would be important to compare the expression (4) with the actual expression of the magnetic susceptibility for a collection of finite chains with random lengths.

Orbital Mechanism of the Exchange in $(Ni(en)_2NO_2)$ Chains

The antiferromagnetic coupling observed in $(Ni(en)_2NO_2)X$ with X = ClO_4, BF_4, PF_6, or I_3 is one of the most important ones reported for fully structurally characterized Ni(II) chains, whereas the nearest intrachain Ni–Ni distance is relatively large, namely, 5.15 Å. The other Ni(II) chains already described that exhibit a large antiferromagnetic coupling are $Ni^{II}L_2$(oxalato) with L = H_2O or a nitrogen-containing ligand ($J \approx -24\ cm^{-1}$)[32] and $ANiX_3$ with A = alkali metal and X = halogen ($-J$ in the range 18–35 cm^{-1}, the record being apparently held by $RbNiCl_3$).[30,33] In this section, we propose to specify the mechanism of the interaction in $(Ni(en)_2NO_2)X$ chains. For that, we shall lean on the orbital model developed in our group[1a] that is valid for chains of transition-metal ions without first-order angular momentum.[19,34] The key expressions of the model are

$$J = J_{AF} + J_F \qquad J_{AF} = \frac{-1}{n^2}\sum_{\mu=1}^{n}\Delta_\mu S_{\mu\mu} \qquad J_F = \frac{2}{n^2}\sum_{\mu,\nu}J_{\mu\nu} \quad (5)$$

where J is the exchange parameter of the isotropic Heisenberg Hamiltonian, which is assumed to be equal to the algebraic sum of a negative antiferromagnetic contribution J_{AF} and a positive ferromagnetic contribution J_F. n is the number of unpaired electrons per metallic center, $S_{\mu\mu}$ is the overlap integral between two magnetic orbitals of the same symmetry μ centered on nearest-neighbor transition-metal ions, Δ_μ is the width of the molecular orbital band constructed from the magnetic orbitals of symmetry μ for the spectroscopic term of highest spin multiplicity, and $J_{\mu\nu}$ is the two-electron exchange integral between magnetic orbitals of symmetry μ and ν, respectively, centered on nearest-neighbor ions. Here a magnetic orbital is defined as a singly occupied orbital centered on a transition-metal ion and partially delocalized toward the ligands surrounding this ion.[35] Finally, at the extended Hückel approximation level, Δ_μ and $S_{\mu\mu}$ are proportional so that J_{AF} varies as $-\Delta_\mu^2$ (or $-S_{\mu\mu}^2$). In the frame of this model, an elegant interpretation of the magnitude of the antiferromagnetic coupling may be proposed. For that, we consider first

(28) C. H. W. Swuste, A. C. Botterman, J. Millenaar, and W. J. M. de Jongh, *J. Chem. Phys.*, **66**, 5021 (1977).
(29) B. N. Bhatia, R. L. Carlin, and A. P. Filho, *Physica B+C (Amsterdam)*, **92B+C**, 330 (1977).
(30) R. Brener, E. Ehrenfreund, H. Shechter, and J. Makovsky, *J. Phys. Chem. Solids*, **38**, 1023 (1977).
(31) See, for instance: W. E. Estes, R. R. Weller, and W. E. Hatfield, *Inorg. Chem.*, **19**, 26 (1980); M. Verdaguer, A. Michalowicz, J. J. Girerd, N. Alberding, and O. Kahn, *Inorg. Chem.*, **19**, 3271 (1980).
(32) C. G. V. Kralingen, J. A. C. Van Ooijen, and J. Reedjik, *Transition Met. Chem. (Weinheim, Ger.)*, **3**, 90 (1978).
(33) H. T. Witteveen and J. A. R. Van Veen, *J. Phys. Chem. Solids*, **35**, 337 (1974).
(34) M. F. Charlot, J. J. Girerd, and O. Kahn, *Phys. Status Solidi*, **B86**, 497 (1978).
(35) O. Kahn and M. F. Charlot, *Nouv. J. Chim.*, **4**, 567 (1980).

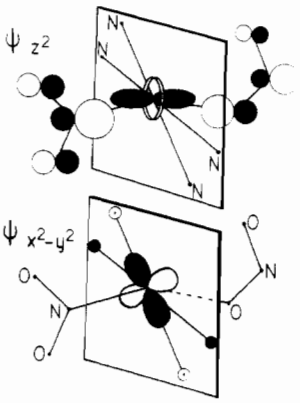

Figure 9. Magnetic orbitals centered on each Ni(II) ion in the $(Ni(en)_2NO_2)$ chain.

the two magnetic orbitals represented in Figure 9 and obtained by extended Hückel calculation on the monomeric fragment shown also in Figure 9.[34,36] The z axis is taken here along the chain axis b. Although the symmetry of the metal site is lower then C_{4v}, the metallic contributions to the magnetic orbitals are almost exclusively $3d_{x^2-y^2}$ for the one and $3d_{z^2}$ for the other one. Thus, it is justified to label these magnetic orbitals $\phi_{x^2-y^2}$ and ϕ_{z^2}, respectively. Examining Figure 8, we can immediately notice that the NO_2^- ligand orbitals do not occur in $\phi_{x^2-y^2}$ but have a large antibonding contribution to ϕ_{z^2}. This magnetic orbital may schematically be described as resulting from the antibonding interaction of $3d_{z^2}$ and of the last occupied MO of each of the NO_2^- ligands, namely the $6a_1$ MO[37] as shown here:

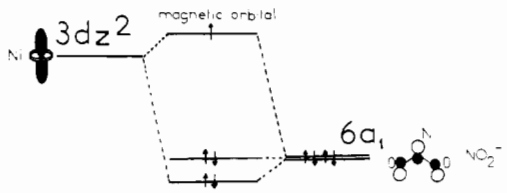

It results from the shape of the magnetic orbitals that the interaction of the $\phi_{x^2-y^2}$'s along the chain will be negligible and that $\Delta_{x^2-y^2}$ will be nearly zero. On the other hand, it is straightforward to see that Δ_{z^2} may be large. Indeed, the two MO's delocalized along the chain and constructed from the ϕ_{z^2}'s corresponding to the top and bottom of the z^2 band are in phase (+ + + +) and out of phase (+ − + −), respectively. The in-phase MO is such that all the metal–NO_2 bridge overlaps are negative. Consequently, this MO will be strongly antibonding with regard to the $3d_{z^2}$ metal orbitals. As for the out-of-phase MO, it is such that the contributions on the bridges tend to cancel themselves so that this MO will be almost nonbonding with regard to the $3d_{z^2}$'s. This situation is schematized in Figure 10.

Considering the interpretation given above, a question may be put, namely, the eventual influence of the O–N–O angle on the magnitude of J_{AF}. An increase of this angle leads to an enhancement of the antibonding π overlap and a lessening of the bonding σ overlap along both N–O bonds. Consequently, the $6a_1$ MO is destablized and its energy is then closer

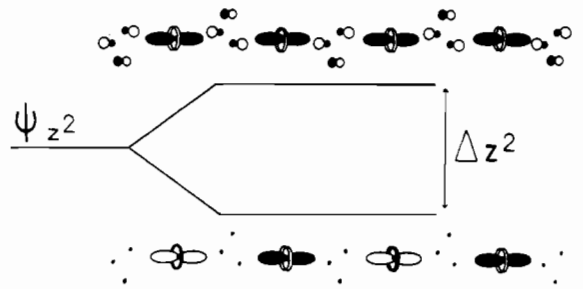

Figure 10. z^2-Type molecular orbital band in the chain $(Ni(en)_2NO_2)$ and in-phase and out-of-phase MO's corresponding to the top and the bottom of the band, respectively.

to that of the $3d_{z^2}$ metal orbital. Therefore, the $3d_{z^2}$–$6a_1$ interaction is enhanced and the contribution of the NO_2^- ligand orbitals in ϕ_{z^2} is more important. It turns out that the in-phase MO will be more antibonding with regard to $3d_{z^2}$ and that Δ_{z^2} will be larger. To summarize, the antiferromagnetic coupling in the chain $(Ni(en)_2NO_2)$ should increase vs. the O–N–O angle of the bridging ligand. To try to check this theoretical prevision, we modified the nature of the counteranion X^- in $(Ni(en)_2NO_2)X$. With the counteranions ClO_4^-, BF_4^-, PF_6^-, and I_3^-, the compounds have actual chain structures. Unfortunately, the O–N–O angle remains practically constant. With the counteranions Cl^-, Br^-, and I^-, the $(Ni(en)_2NO_2)$ species are monomeric.[38] With the tetraphenylborate anion, a new compound of $(Ni(en)_2NO_2)BPh_4$ stoichiometry was obtained; its quite unusual structure will be described in a forthcoming paper.[39]

It is perhaps important here to emphasize that the relations (5) do not mean in any way that the electronic structure of the insulating one-dimensional magnetic compounds may be described in the framework of the band model. Δ_μ is the energy difference between the highest and the lowest MO's for the only state of highest spin multiplicity. For any low-lying state, the appropriate wave functions are of Heitler–London type and describe electrons localized in the magnetic orbitals. For the state of highest spin multiplicity, the Heitler–London wave functions are strictly identical with the MO wave functions.

Conclusions

In this work, we showed that the bridging ligand NO_2^- can transmit the electronic effects between Ni(II) ions relatively far away from each other in a particularly efficient fashion. This is realized when the $6a_1$ HOMO's of each NO_2^- bridge are properly orientated regarding the orientations of the singly occupied metal orbitals. In $(Ni(en)_2NO_2)$ chains, the strong antiferromagnetic coupling between Ni(II) ions separated by 5.15 Å is due to the importance in absolute value of the term $\Delta_{z^2}S_{z^2,z^2}$ in the expression of J given in (5). As a matter of fact, we have from (5)

$$\Delta_{z^2}S_{z^2,z^2} + \Delta_{x^2-y^2}S_{x^2-y^2,x^2-y^2} > 4|J|$$

Hence, since $\Delta_{x^2-y^2}S_{x^2-y^2,x^2-y^2}$ is negligible, $\Delta_{z^2}S_{z^2,z^2} > 4|J|$ (namely, 132 cm^{-1} in the perchlorate derivative). The overlap S_{z^2,z^2} between ϕ_{z^2} magnetic orbitals centered on nearest-neighbor Ni(II) ions is favored owing to the spatial orientations of the HOMO's $6a_1$ for the two NO_2^- ligands bound to a same metal ion. The large energy gap Δ_{z^2} between the top and the bottom of the band of the chain molecular orbitals constructed from the ϕ_{z^2} magnetic orbitals results from the importance of S_{z^2,z^2}. The top of the band corresponds to a MO strongly

(36) To determine the magnetic orbitals shown in Figure 8, we use a version of the EH program with charge iteration, Madelung correction for the potential, and weighted H_{ij}. The atomic orbitals are simple Slater-type orbitals with Burns' exponent for N and O atoms and two-component orbitals with Richardson's exponents for Ni(II) ions. The A_μ, B_μ, C_μ, and $g_{\mu\mu}$ parameters come from version 8 of the ICON program distributed by QCPE (program no. 344). The K parameter of the Wolfsberg–Helmholz approximation is taken equal to 1.75.

(37) J. F. Wyatt, I. H. Hillier, V. R. Saunders, J. A. Connor, and M. Barber, *J. Chem. Phys.*, **54**, 5311 (1971).

(38) B. M. Chedrine, I. V. Belov, I. P. Jidkov, M. A. Porai-Koshits, and A. E. Chvelachvili, *Dokl. Akad. Nauk SSSR*, **170**, 1312 (1966).

(39) A. Gleizes, A. Meyer, M. A. Hitchman, and O. Kahn, *Inorg. Chem.*, in press.

antibonding with regard to the metal d_{z^2} orbitals while the bottom corresponds to an essentially nonbonding interaction of the d_{z^2} metal orbital. The z^2 exchange pathway that occurs in the compounds investigated in this paper as well as in other compounds where octahedral chromophores share either opposite corners or opposite trigonal faces[30,33] appears to be one of the most efficient for Ni(II) coupled systems. In particular, it leads to stronger antiferromagnetic interactions than the $x^2 - y^2$ exchange pathway, which predominates when octahedral chromophores share opposite edges.[21,28] In contrast, it is now well established that the x^2–y^2 exchange pathway is particularly efficient in Cu(II) coupled systems.[2-4,35,40]

Acknowledgment. This work was technically and financially supported by the CNRS, the DGRST, and the DESR.

Registry No. $Ni(N_2C_2H_8)_2(NO_2)(PF_6)$, 80642-84-8; $Ni(N_2C_2H_8)_2(NO_2)(ClO_4)$, 30496-54-9; $Ni(N_2C_2H_8)_2(NO_2)(I_3)$, 80642-85-9.

Supplementary Material Available: Listings of structure factor amplitudes (5 pages). Ordering information is given on any current masthead page.

(40) J. J. Girerd, O. Kahn, and M. Verdaguer, *Inorg. Chem.*, **19**, 274 (1980).

Contribution from the Department of Chemistry,
University of Notre Dame, Notre Dame, Indiana 46556

Triborane. A Transition-Metal Ligand or Heterocluster Fragment?

CATHERINE E. HOUSECROFT and THOMAS P. FEHLNER*

Received October 5, 1981

The nature of the metal–boron bonding in three metallaboranes containing triborane fragments possessing significantly different geometrical structures is explored by means of the extended Hückel technique. It is demonstrated that important aspects of the nature of the structures of these three metallaboranes can be understood on the basis of the frontier orbital behavior of the triborane fragments as a function of triborane geometry. This work confirms the relationship of one metallaborane to organometallic allyl complexes and explores the ligand behavior of the $B_3H_8^-$ ion toward metals. In addition a trend in ligand vs. cluster behavior for the three triborane fragments is established.

Introduction

It is well established that boranes can serve as ligands to metals in low-valence states in a manner parallelling organic fragments.[1] Moreover, metallaboranes have been classified according to the ligand behavior of the borane fragment with respect to the metal.[2] On the other hand, metallaboranes can be usefully considered as clusters, a description also encompassing organometallic compounds.[3] The difference between the two views is partly semantic, but it is of interest to explore the implied real differences in terms of metallaboranes containing the same size borane fragment in dissimilar bonding arrangements.

The triborane fragment is the simplest polyborane in which three distinct bonding modes toward metal are exhibited. These are distinguished by significant changes in the geometry of the borane fragment as established crystallographically. In the first mode, of which $(Me_2PPh)_2PtB_3H_7$ is the exemplar,[4] the triborane, B_3H_7, binds to the metal in a structural form analogous to the allyl cation ($C_3H_5^+$), hence the term "borallyl" (Figure 1). Further evidence for this bonding mode comes from NMR studies of $Ir(B_3H_7)(CO)H(PPh_3)_2$.[5] The bonding of larger borane fragments to transition metals via three borons has also been described as allyl-like.[6] The second known form of triborane bonding to transition metals is found in compounds containing $B_3H_8^-$, a species that can be isolated as uncomplexed ligand as well.[7] Structurally characterized examples include $(Ph_3P)_2CuB_3H_8$,[8] $[(CO)_4CrB_3H_8]^-$,[9] $(CO)_4MnB_3H_7Br$,[10] and $Be(B_3H_8)_2$.[11,12] The bonding in the first three has been likened to that of the *nido*-borane, B_4H_{10}, in which the metal fragment replaces a "wing-tip" BH_2^+ in the borane "butterfly" (Figure 2).[1] Note that $B_3H_8^-$ can be formally generated from B_3H_7 by the addition of H^- to the central boron. The third established bonding mode for triboranes is found in the ferraborane, $(CO)_6Fe_2B_3H_7$, a formal dimetallapentaborane[13] (Figure 3). The triborane ligand is positioned such that all three boron atoms are associated with the apical iron atom, while two basal borons are associated with the remaining iron via two bridging hydrogens. The binding of this triborane to a diiron fragment has been examined earlier,[13,14] and it is clear that the most useful description of the structure of this compound is as a formal derivative of B_5H_9; i.e., neither the borallyl nor the $B_3H_8^-$ descriptions serve as good models. This is most dramatically evidenced by the BBB angle of the triborane being 113° in the borallyl compound, 60° in the $B_3H_8^-$, derivatives and 94° in this ferraborane.

In this work we explore these three distinct binding modes exhibited by triboranes using qualitative molecular orbital methods in the manner of Hoffmann.[15] By considering the compounds containing triborane as being formed from appropriate metal and borane fragments, it is possible to examine

(1) Dunks, G. B.; Hawthorne, M. F. In "Boron Hydride Chemistry"; Muetterties, E. L., Ed.; Academic Press: New York, 1975; p 383. Wegner, P. A. *Ibid.*, p 431.
(2) Greenwood, N. N. *Pure Appl. Chem.* **1977**, *49*, 791.
(3) Wade, K. *J. Chem. Soc., Chem. Commun.* **1971**, 792. Mingos, D. M. P. *Nature (London), Phys. Sci.* **1972**, *236*, 99. Rudolph, R. W. *Acc. Chem. Res.* **1976**, *9*, 446. Grimes, R. N. *Ibid.* **1978**, *11*, 420.
(4) Guggenberger, L. J.; Kane, A. R.; Muetterties, E. L. *J. Am. Chem. Soc.* **1972**, *94*, 5665.
(5) Greenwood, N. N.; Kennedy, J. D.; Reed, D. *J. Chem. Soc., Dalton Trans.* **1980**, 196.
(6) Hilty, T. K.; Thompson, D. A.; Butler, W. M.; Rudolph, R. W. *Inorg. Chem.* **1979**, *18*, 2642.
(7) Peters, C. R.; Nordman, C. E. *J. Am. Chem. Soc.* **1960**, 82, 5738.
(8) Lippard, S. J.; Melmed, K. M. *Inorg. Chem.* **1969**, *8*, 2755.
(9) Guggenberger, L. J. *Inorg. Chem.* **1970**, *9*, 367.
(10) Chen, M. W.; Calabrese, J. C.; Gaines, D. R.; Hillenbrand, D. F. *J. Am. Chem. Soc.* **1980**, *102*, 4928.
(11) Calabrese, J. C.; Gaines, D. F.; Hildebrandt, S. J.; Morris, J. H. *J. Am. Chem. Soc.* **1976**, *98*, 5489.
(12) Other modes of bonding of the $B_3H_8^-$ species such as tridentate (Hildebrandt, S. J.; Gaines, D. F.; Calabrese, J. C. *Inorg. Chem.* **1978**, *17*, 790) or as a dimetal bridge (Chen, M. W.; Gaines, D. F.; Hoard, L. G. *Ibid.* **1980**, *19*, 2989) have been observed.
(13) Haller, K. J.; Andersen, E. L.; Fehlner, T. P. *Inorg. Chem.* **1981**, *20*, 309.
(14) Andersen, E. L.; DeKock, R. L.; Fehlner, T. P. *Inorg. Chem.* **1981**, *20*, 3291.
(15) Hoffman, R. *Science (Washington, D.C.)* **1981**, *211*, 995 and references therein.

0020-1669/82/1321-1739$01.25/0